# Planetary Wave Breaking and Tropospheric Forcing as Seen in the Stratospheric Sudden Warming of 2006

LAWRENCE COY, STEPHEN ECKERMANN, AND KARL HOPPEL

*Naval Research Laboratory, Washington, D.C.*

(Manuscript received 7 March 2008, in final form 25 July 2008)

ABSTRACT

The major stratospheric sudden warming (SSW) of January 2006 is examined using meteorological fields from Goddard Earth Observing System version 4 (GEOS-4) analyses and forecast fields from the Navy Operational Global Atmospheric Prediction System–Advanced Level Physics, High Altitude (NOGAPS-ALPHA). The study focuses on the upper tropospheric forcing that led to the major SSW and the vertical structure of the subtropic wave breaking near 10 hPa that moved low tropical values of potential vorticity (PV) to the pole. Results show that an eastward-propagating upper tropospheric ridge over the North Atlantic with its associated cold temperature perturbations (as manifested by high 360-K potential temperature surface perturbations) and large positive local values of meridional heat flux directly forced a change in the stratospheric polar vortex, leading to the stratospheric subtropical wave breaking and warming. Results also show that the anticyclonic development, initiated by the subtropical wave breaking and associated with the poleward advection of the low PV values, occurred over a limited altitude range of approximately 6–10 km. The authors also show that the poleward advection of this localized low-PV anomaly was associated with changes in the Eliassen–Palm (EP) flux from equatorward to poleward, suggesting an important role for Rossby wave reflection in the SSW of January 2006. Similar upper tropospheric forcing and subtropical wave breaking were found to occur prior to the major SSW of January 2003.

## 1. Introduction

Sudden stratospheric warmings (SSWs) are a major component of the stratospheric circulation. Over the course of a few days the wintertime westerly stratospheric polar vortex is disrupted and the midstratospheric temperatures in the polar night increase rapidly by as much as 60 K (see Andrews et al. 1987). These dramatic changes are produced when strong planetary-scale Rossby wave forcing in the troposphere leads to Rossby wave breaking and dissipation in the stratosphere (see Haynes 2005). In this paper we examine both the tropospheric forcing and the Rossby wave breaking that occurred during the major SSW of January 2006.

There are still some questions about the tropospheric forcing of SSWs. As noted by Taguchi (2008), it has been assumed that SSWs are forced by large-scale tropospheric events such as blocking. However, a study of 49 yr of reanalysis data by Taguchi (2008) showed no statistically significant correlation between tropospheric blocking events and SSWs, implying that not all SSWs are forced by blocking events. Smaller-scale transient Rossby waves are generally not considered because the Charney–Drazin criterion (Charney and Drazin 1961, hereafter CD61) limits the propagation of small-scale waves in the stratosphere. However, as noted by Haynes (2005), the Charney–Drazin result is derived under the assumptions of small-amplitude waves on a slowly varying (in the vertical) background flow. Additionally, wave transience is not considered in CD61. If the restrictions of CD61 are not met, then smaller-scale transient disturbances in the troposphere may play a role in forcing some SSWs. In this paper we examine the scale and duration of the tropospheric forcing that led directly to the SSW of January 2006.

The mechanism of the SSW relies on the nonlinear breaking of upward-propagating Rossby waves, either through wave amplitude increase with decreasing density (Polvani and Saravanan 2000) or interaction with a critical layer (Killworth and McIntyre 1985). In

*Corresponding author address:* Lawrence Coy, Space Science Division, Naval Research Laboratory, Code 7646, 4555 Overlook Avenue, SW, Washington, DC 20375.
E-mail: coy@nrl.navy.mil

DOI: 10.1175/2008JAS2784.1

# Report Documentation Page

*Form Approved*
*OMB No. 0704-0188*



| 1. REPORT DATE | 2. REPORT TYPE | 3. DATES COVERED |
|---|---|---|
| **FEB 2009** | | **00-00-2009 to 00-00-2009** |

| 4. TITLE AND SUBTITLE | 5a. CONTRACT NUMBER |
|---|---|
| **Planetary Wave Breaking and Tropospheric Forcing as Seen in the Stratospheric Sudden Warming of 2006** | 5b. GRANT NUMBER |
| | 5c. PROGRAM ELEMENT NUMBER |
| 6. AUTHOR(S) | 5d. PROJECT NUMBER |
| | 5e. TASK NUMBER |
| | 5f. WORK UNIT NUMBER |
| 7. PERFORMING ORGANIZATION NAME(S) AND ADDRESS(ES) **Naval Research Laboratory,Washington,DC** | 8. PERFORMING ORGANIZATION REPORT NUMBER |
| 9. SPONSORING/MONITORING AGENCY NAME(S) AND ADDRESS(ES) | 10. SPONSOR/MONITOR'S ACRONYM(S) |
| | 11. SPONSOR/MONITOR'S REPORT NUMBER(S) |

12. DISTRIBUTION/AVAILABILITY STATEMENT
**Approved for public release; distribution unlimited**

13. SUPPLEMENTARY NOTES

14. ABSTRACT

15. SUBJECT TERMS

| 16. SECURITY CLASSIFICATION OF: | | | 17. LIMITATION OF ABSTRACT | 18. NUMBER OF PAGES | 19a. NAME OF RESPONSIBLE PERSON |
|---|---|---|---|---|---|
| a. REPORT **unclassified** | b. ABSTRACT **unclassified** | c. THIS PAGE **unclassified** | **Same as Report (SAR)** | **14** | |

particular, Rossby waves that propagate meridionally toward the weak tropical stratospheric winds can break dramatically (subtropical wave breaking), triggering irreversible transport of tropical air to middle latitudes (Randel et al. 1993; Waugh 1993; Polvani et al. 1995). In the modeling study of Polvani and Saravanan (2000), the vertical scale of Rossby wave breaking at the vortex edge was characterized as deep. However, for the case of subtropical wave breaking, the mainly horizontally propagating Rossby waves may be limited in vertical extent and consequently may have more vertically limited wave breaking. This would imply that strong mixing between the subtropics and tropics would also be limited in its vertical extent as well. In addition, although poleward focusing of wave activity is seen in composite SSW studies (e.g., Limpasuvan et al. 2004), there is still a question of the importance of wave reflection from the subtropical critical layer in the poleward focusing of the wave activity (Dunkerton et al. 1981). In this paper we examine the vertical scale of the subtropical wave breaking as seen in the SSW of January 2006 and the poleward focusing due to the nonlinear poleward transport of tropical air.

The plan of this paper is to start with a brief description of the analyses and forecast model used in the study (section 2). Next we examine the tropospheric forcing of the January 2006 SSW using the meteorological analyses along with forecast model experiments showing the dependence of a realistic SSW forecast on correctly forecasting the tropospheric forcing (section 3). This is followed by an examination of the vertical structure of the wave breaking event (section 4). The final section provides some additional discussion and a summary (section 5).

## 2. Analyses and forecast model

In this study, we use Goddard Earth Observing System version 4 (GEOS-4; Bloom et al. 2005) assimilated meteorological fields. The global GEOS-4 analyses were available every 6 h on a 1.25° × 1° longitude–latitude grid at 36 pressure levels, from 1000 to 0.2 hPa. The time period examined covered January–February 2006.

To explore the dependence of the major stratospheric warming on tropospheric forcing, we also use analyses and forecasts based on a high-altitude version of the Navy's operational global forecast and data assimilation system, the Navy Operational Global Atmospheric Prediction System (NOGAPS; Hogan and Rosmond 1991; Goerss and Phoebus 1992)–Advanced Level Physics, High Altitude (ALPHA; Eckermann et al. 2004, 2008; McCormack et al. 2004). In this paper, NOGAPS-ALPHA was run at T79 and T239 triangular wavenumber truncations (~2.25° and ~0.75° resolution, respectively), with 68 vertical levels, ~2-km vertical resolution in the stratosphere, and a model top at 0.0005 hPa (~100 km). More details on this configuration can be found in Hoppel et al. (2008).

## 3. Tropospheric forcing

A major SSW occurred on 20 January 2006. At this time, the zonal-mean zonal winds at 10 hPa and 60°N switched from westerly to easterly. The next day, temperatures at the winter pole rose from 230 K to over 260 K. The 1100-K (just above 10 hPa) potential vorticity (PV) field during this warming event is shown in Fig. 1 at selected times. The vortex was off the pole and relatively stationary during 12–14 January; however, by 16 January the orientation of the vortex had changed (propagated east) and strong subtropical wave breaking had begun. By 20 January normally tropical values of PV formed an anticyclonic circulation at 60°N, creating the major warming. On subsequent days this low-PV anomaly moved across the pole.

The synoptic development of the upper tropospheric forcing and middle stratosphere response is shown in Fig. 2, which depicts geopotential heights at 10 and 200 hPa over the North Atlantic region on 15–18 January 2006. (Note: for clarity, only two contours are shown at 200 hPa.) The 200-hPa heights show a large eastward-propagating ridge that forms over the North Atlantic (~45°W) during this time. This ridge develops its largest amplitude, in terms of both poleward and longitudinal extent, on 16–17 January. The eastward phase speed is ~12 m $s^{-1}$.

At 10 hPa the vortex orientation (or longitudinal phase) is changing over 15–18 January. This change in orientation seen in Fig. 2 can also be seen in the PV fields (see Fig. 1, in which 0° longitude is located at the bottom). From 14–16 January the orientation of the vortex changes by rotating to the east and moving closer to the tropics. At this time (16 January) the sudden warming begins as tropical air is rapidly pulled northward. Note in Fig. 2 how the change in the orientation of the 10-hPa heights from 15–16 January closely follows the developing ridge at 200 hPa.

Also plotted in Fig. 2 is the height of the 360-K potential temperature surface. (Note: for clarity only the lowest and highest contours are shown.) A high of over 14.5 km is found on 16–17 January 2006, associated with warm air in the lower troposphere that is being advected around the surface high pressure system (not shown). A high 360-K surface indicates cold air in the upper troposphere. The average value of the 360-K surface at

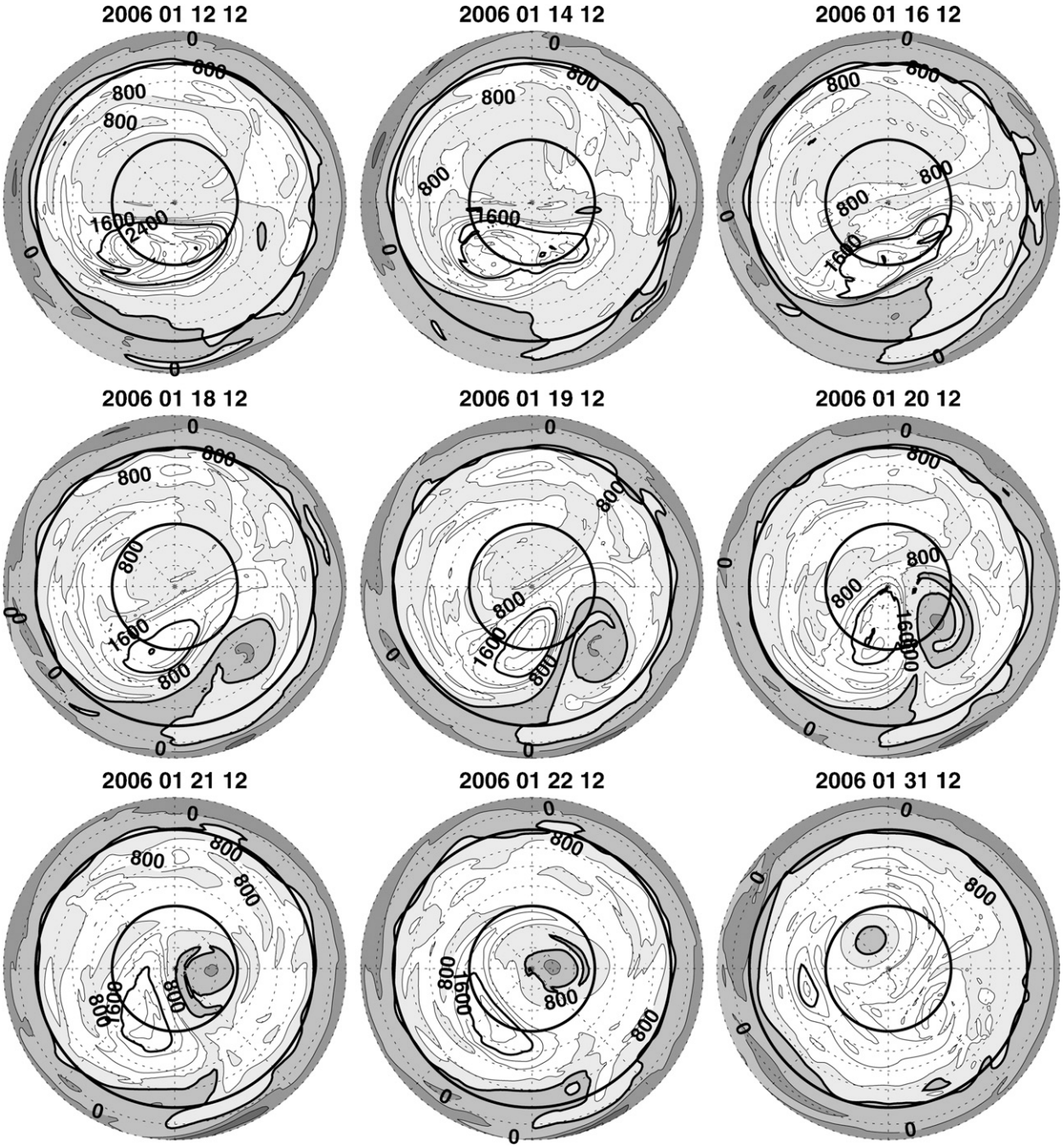


FIG. 1. Potential vorticity (PVU) at 1100 K on 12, 14, 16, 18, 19, 20, 21, 22, and 31 Jan 2006. Map projection is Lambert equal area from equator to North Pole. Bold circles are at 20° and 60° north. The Greenwich meridian is at the bottom of the figures (0° longitude). The contour interval is 400 PVU. Dark shading denotes low PV. Dates on each panel are given as year, month, day, and hour (UTC).

50°N over January–February 2006 is 12.25 km. To the extent that the 360-K surface approximates a material surface, these 360-K heights of more than 2 km above the average can be expected to have a large dynamical effect on the stratospheric jet flowing over this disturbance.

Figure 3 shows the time dependence of some indicators of the tropospheric disturbance at 50°N. The large maximum in 360-K potential temperature surface heights (Fig. 3a) occurs before the warming on 16–17 January 2006 and coincides with a large maximum in the local meridional heat flux ($v'T'$; Fig. 3b) and with a strong

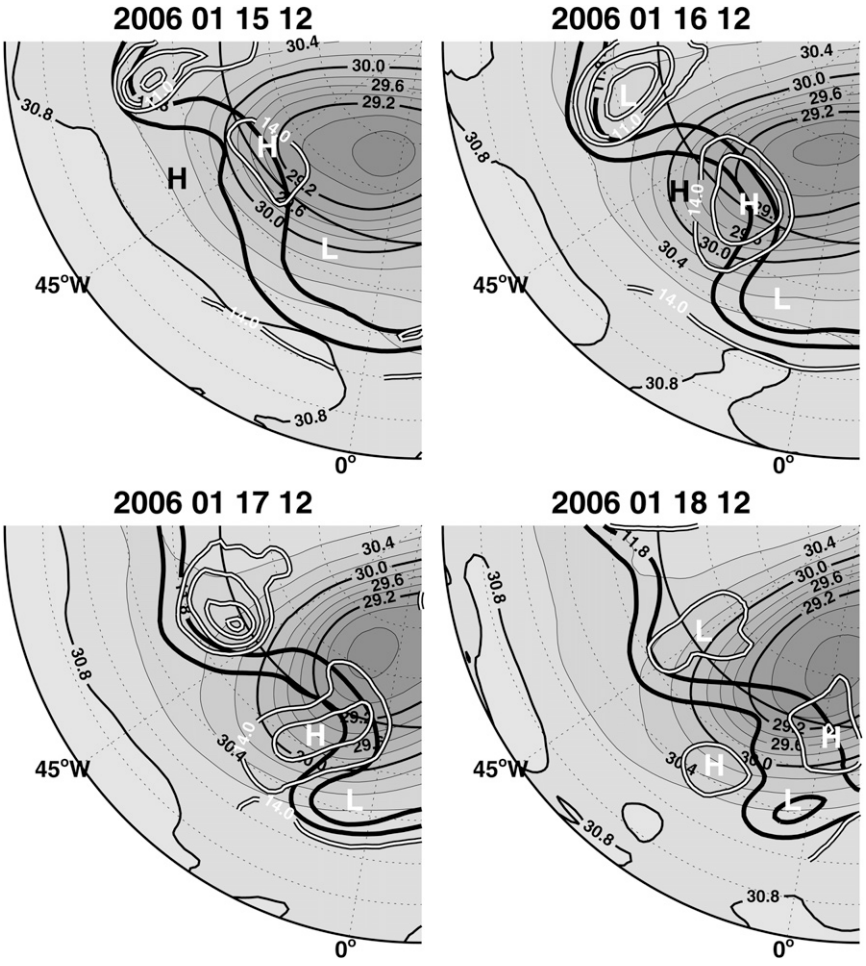


FIG. 2. The 10-hPa geopotential heights (shaded contours), contour interval 0.2 km, darker shading denotes lower heights; 200-hPa geopotential heights contoured at 11.8 and 12 km (thick black contours); and 360-K potential temperature surface heights at 10, 10.5, 11, 11.5, 14, 14.5 km (white contours) on (top) (left) 15 and (right) 16, and (bottom) (left) 17 and (right) 18 Jan 2006. Map projection is Lambert equal area from equator to North Pole showing a quadrant from 80°W to 10°E. Bold latitudes are at 0° and 50°N.

minimum in the 100-hPa temperatures (Fig. 3c). (Note that the meridional heat flux in Fig. 3b is the local product of the meridional wind and temperatures with their respective zonal averages removed.) Figure 3d plots the maximum 150-hPa geopotential heights found at each time and shows a peak on 16 January, before the SSW. Note, however, that other large peaks in the upper tropospheric heights occurring throughout the January–February time period are not accompanied by SSWs, implying that the magnitude of the upper tropospheric geopotential heights is not as good an indicator of the forcing as the quantities plotted in Figs. 3a–c. These local extreme values seen in Figs. 3a–d are all occurring over the North Atlantic on 15–19 January. The zonally averaged meridional heat flux ($\overline{v'T'}$; Fig. 3e) shows a maximum on 16 January; however, like the upper tropospheric geopotential heights, this peak is not much greater than later peaks. Thus, local quantities based on upper tropospheric temperature and meridional wind (such as Figs. 3a–c) are the best indicators of the large upper tropospheric disturbance.

Figure 4 shows the time dependence of some indicators of the stratospheric response to the tropospheric forcing. The local momentum flux at 45°N ($u'v'$, Fig. 4a) increases on 16–17 January, followed by a peak on 19 January. This peak value is located over the North Atlantic sector. The zonally averaged momentum flux at 45°N ($\overline{u'v'}$; Fig. 4a) shows a similar time dependence, peaking on 19 January. The warming at the pole (Fig. 4c) occurs later, on 21 January. Thus, the strongest

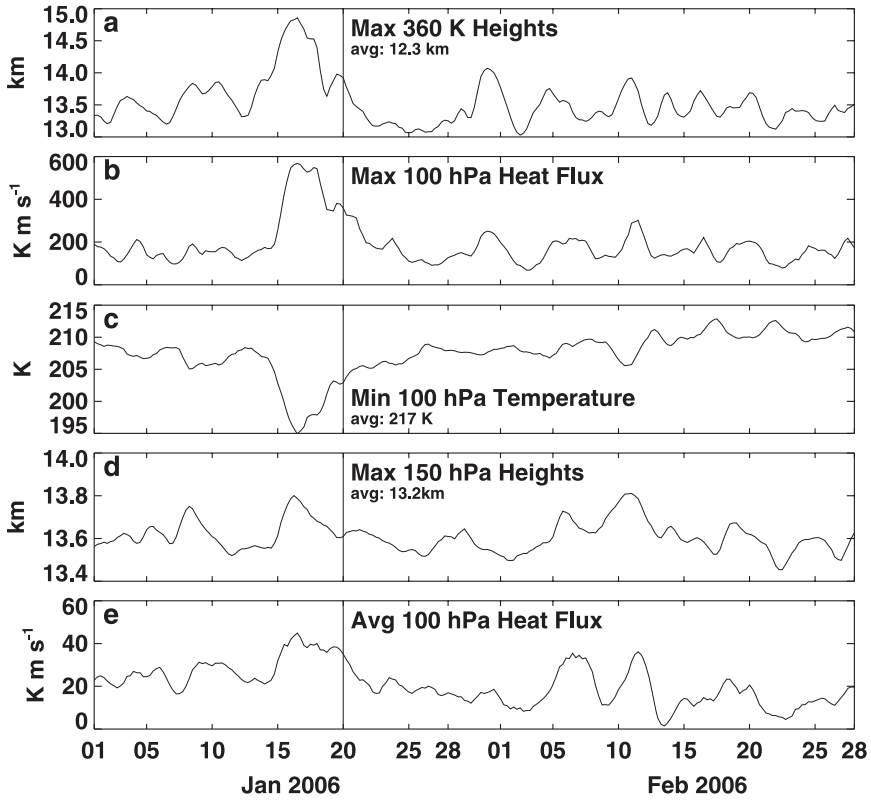


FIG. 3. Time series at 50°N for (a) the maximum value of the 360-K potential temperature surface height (km), (b) the maximum value of the 100-hPa meridional heat flux, $v'T'$ (K m s$^{-1}$), (c) the minimum temperature at 100 hPa (K), (d) the maximum value of the 150-hPa geopotential heights (km), and (e) the zonally averaged 100-hPa meridional heat flux, $\overline{v'T'}$(K m s$^{-1}$). The maxima and minimum are with respect to all longitudes at 50°N.

midstratospheric momentum flux response occurs after the strong tropospheric forcing.

Figure 5 shows the Northern Hemisphere distribution of the 100-hPa meridional heat flux and 450-K PV on 16 January 2006. The large meridional heat flux in the North Atlantic is seen to develop under the lower stratospheric vortex edge. This meridional heat flux pattern corresponds closely with the cold temperatures at 100 hPa and the high 360-K potential temperature surface heights. Note that the meridional heat flux over the North Atlantic is the only significant feature at 100 hPa at this time.

Figure 6 shows geopotential height perturbations as a function of altitude at 50°N for 15–18 January 2006. During this time period both the tropospheric high pressure ridge and the stratospheric low move eastward together at ~30°W. Figure 6 shows that not just the 10-hPa heights but heights at all stratospheric altitudes move with the tropospheric high. From 15–17 January, the vertical structure is close to being equivalent barotropic from the surface up to the stratopause in the region of the tropospheric high. However, by 18 January a westward tilt with altitude, characteristic of vertically propagating planetary waves, is beginning to appear in the stratosphere.

In a zonally averaged picture, the meridional heat flux and the horizontal momentum flux can be combined into the Eliassen–Palm (EP) flux (see Andrews et al. 1987, p. 128). Plotting the EP flux vectors in a latitude/height section shows the magnitude and direction of wave activity propagation. Figure 7 shows the zonally averaged zonal wind and EP flux vectors for 15–18 January 2006. The EP flux vectors in the troposphere show large divergences at 200 hPa and 45–50°N on 16 and 17 January, which lead to the increase in EP flux magnitude at 10 hPa on 18 January. The large EP flux divergence indicates a wave source in the upper troposphere. Figure 7 also shows that the equatorial component of the EP flux has increased by 18 January, extending equatorward of 30°N, in agreement with the increase in momentum flux seen in Fig. 4. Note that the zonally averaged zonal wind in the tropics is westerly

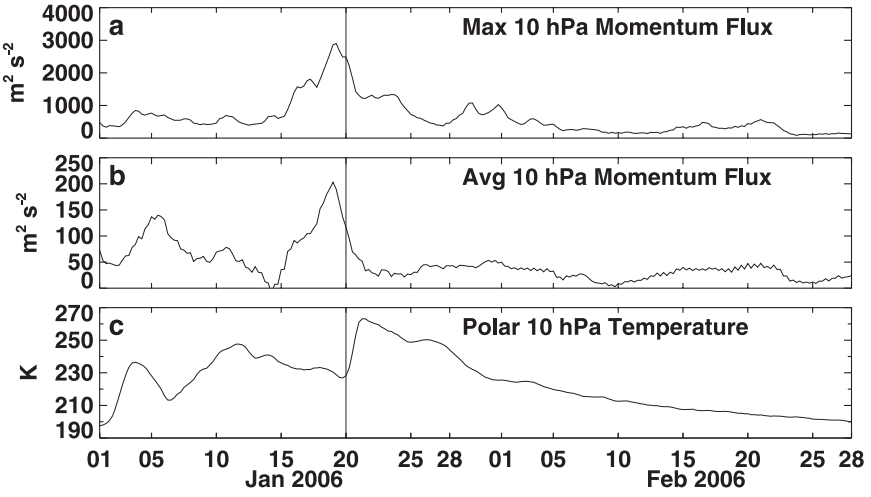


FIG. 4. Time series at 10 hPa for (a) the maximum value of the momentum flux $u'v'$ ($m^2\ s^{-2}$) at 45°N, (b) the zonally averaged momentum flux $\overline{u'v'}$ ($m^2\ s^{-2}$) at 45°N, and (c) the temperature (K) at 90°N. The maximum is with respect to all longitudes at 45°N.

near 10 hPa, allowing the nearly stationary Rossby waves to propagate deep into the tropics at 10 hPa before encountering their critical layer.

The dependence of the January 2006 SSW on upper tropospheric forcing over the North Atlantic was examined by initializing a forecast model at different times before the upper tropospheric forcing event. These experiments were similar to those performed by Allen et al. (2006) for the 2002 Southern Hemisphere SSW. The results are presented in Fig. 8, which plots diagnostics for the stratospheric warming and upper tropospheric forcing.

The two forecasts initialized on 13 January 00 UTC predict an increase in maximum 360-K potential temperature heights but underestimate the magnitude (Fig. 8). Neither the low–horizontal resolution forecast (T79, ~2.25° resolution), nor the high–horizontal resolution forecast (T239, ~0.75° resolution) predicts the high 10-hPa polar temperatures seen in the analysis. However, Figs. 8b and 8c show that the higher–horizontal resolution forecast better predicts the 16–17 January maximum 360-K potential temperature heights and anomaly area than the lower-resolution forecast. The T79 forecast initialized on 15 January does predict

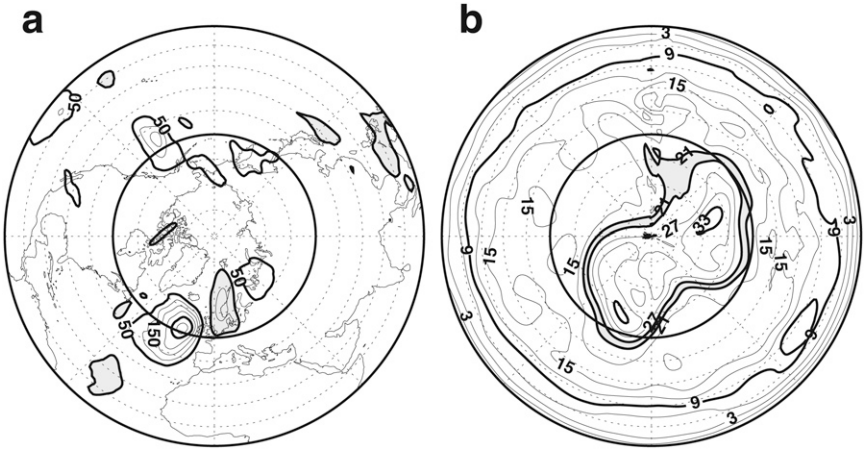


FIG. 5. Lambert equal area projection from equator to North Pole on 1200 UTC 16 Jan 2006 showing (a) meridional heat flux $v'T'$ (contour interval of 50 K m $s^{-1}$) at 100 hPa and (b) PV at 450 K (contour interval of 3 PVU). Bold latitudes are at 0° and 50°N.

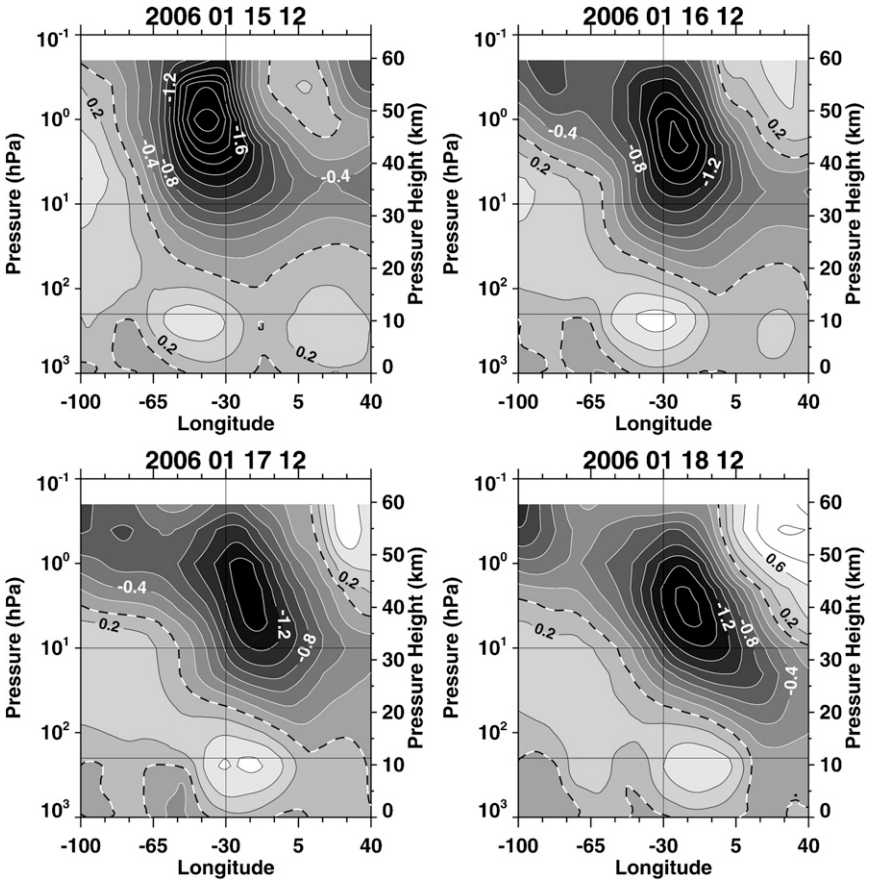


FIG. 6. Geopotential height perturbations from the zonal average (contour interval, 0.2 km) on 15, 16, 17, and 18 Jan 2006 as a function of longitude and pressure at 50°N. White contours denote negative perturbations. The zero contour is dashed. Longitudes are from 100°W to 40°E. The 10- and 200-hPa pressures are denoted by horizontal lines.

a polar warming on 21 January that is close to the observed polar temperature on 22 January. Although the maximum 360-K values for the forecast initialized on 15 January are not much greater than the high-resolution 13 January initialization forecasts (Fig. 8b), the anomaly area is much closer to the values seen in the analysis (Fig. 8c). The T79 forecast initialized on 17 January, the time of the maximum of the 360-K potential temperature heights and anomaly area, also predicts the major warming on 22 January, with a polar temperature about 5 K higher than seen in the analyses. Thus, a realistic forecast of the upper tropospheric forcing is necessary for the model to forecast the major SSW of January 2006.

In summary, an upper tropospheric disturbance amplified dramatically on 16–17 January 2006 as the tropospheric ridge system in the North Atlantic propagated under the lower (460 K) and mid (1100 K)-stratospheric jet. This amplification extended into the midstratosphere and was associated with strong upward displacement of the 360-K potential temperature surface and production of strong vertical EP flux. This was followed on 19 January by increased equatorward Rossby wave propagation at ~10 hPa, resulting in a large subtropical wave breaking event. The subsequent nonlinear advection of low values of PV from the tropics to the pole then generated the SSW (20–21 January).

## 4. Vertical structure of the wave breaking event

In this section we examine the vertical structure associated with subtropical wave breaking and the change in sign of the horizontal component of the EP flux. We begin by examining vertical cross sections of the poleward transport of low PV that resulted from the wave breaking. Instead of plotting vertical cross sections of scaled PV (e.g., Lait 1994), here we simply plot absolute vorticity, a quantity that has the mean latitudinal gradient of interest. The minimum absolute vorticity at

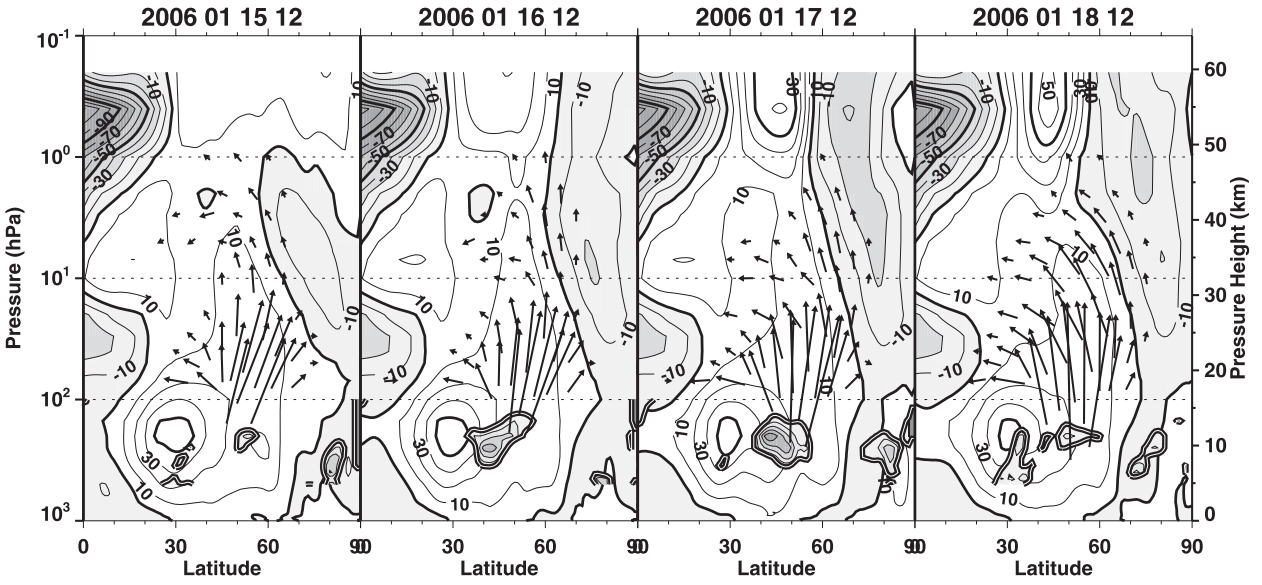


FIG. 7. The zonal average of zonal wind for 15, 16, 17, and 18 Jan 2006. Contour interval 10 m $s^{-1}$; easterly winds are shaded. Arrows denote EP flux vectors plotted above the tropopause. Double line contour denotes tropospheric regions of strong EP flux divergence.

each latitude and pressure serves as an accurate proxy for the single low-PV anomaly during late January 2006.

Figure 9 shows that the isolated region of low absolute vorticity associated with the PV anomaly is centered just below 1100 K on 19–20 January and is moving poleward. By 22 January the low-PV feature is centered at 1100 K and is near the pole. At later times, such as 31 January, the feature is located midway between 1100 and 800 K and has weakened somewhat. During the poleward advection, the vertical width of the absolute vorticity anomaly (minimum PV representative of minimum values typically found at 20°N) increases from ~6 to ~10 km. The minimum value of absolute vorticity associated with the PV anomaly remains almost constant during its rapid poleward transit (19, 20, and 22 January panels in Fig. 9), suggesting that absolute vorticity is well conserved in the PV anomaly and implying that vortex stretching and tilting in the PV anomaly are secondary effects during this time. However, the PV anomaly is somewhat weaker by 31 January. Note that the anomaly carries absolute vorticity values typical of ~15°N to the pole. As expected from the near conservation of absolute vorticity in this case, the relative vorticity (not shown) decreases during this rapid poleward transport. Also shown in Fig. 9 are the zonally averaged potential temperatures. By 22 January, the 850- and 1100-K potential temperature surfaces have become depressed near the pole indicating polar warming induced by the PV anomaly.

The low-PV anomaly can be expected to influence the zonally averaged winds and EP flux vectors as the anomaly moves poleward. Figure 10 shows latitude–height cross sections of the zonally averaged zonal wind and EP flux vectors. As the PV anomaly propagated poleward, the anticyclonic circulation about it increased. This can be seen in Fig. 10 in the 20 January 2006 panel as westerly winds poleward of the PV anomaly and easterly winds eastward of the PV anomaly at ~10 hPa and above. The EP flux vectors in Fig. 10 show that planetary waves are propagating into the weak tropical wind region located just above 10 hPa on 19 and 20 January. The EP flux vectors tend to follow the motion of the PV anomaly over 19–22 January, with the EP flux vectors at 10 hPa becoming more vertical (19–20 January) and finally pointing slightly poleward at the height of the warming (22 January). Although wave activity continues to propagate upward during this time, reflection of wave activity from the subtropical wave breaking region appears responsible for the polar focusing. After the polar warming (31 January), westerly winds continue to descend. The EP flux is reduced at this time and is limited in vertical extent by the polar easterlies.

Note that the sign of the zonally averaged momentum flux (and thus the meridional direction of Rossby wave propagation) can be inferred from Fig. 1 for this warming event because the strongest flow is between the high-PV polar vortex and the low poleward-moving PV anomaly. On 18 January the flow is mainly out of the tropics from southwest to northeast. However, by 22 January, the strong flow poleward of 60°N is now oriented from southeast to northwest. These strong

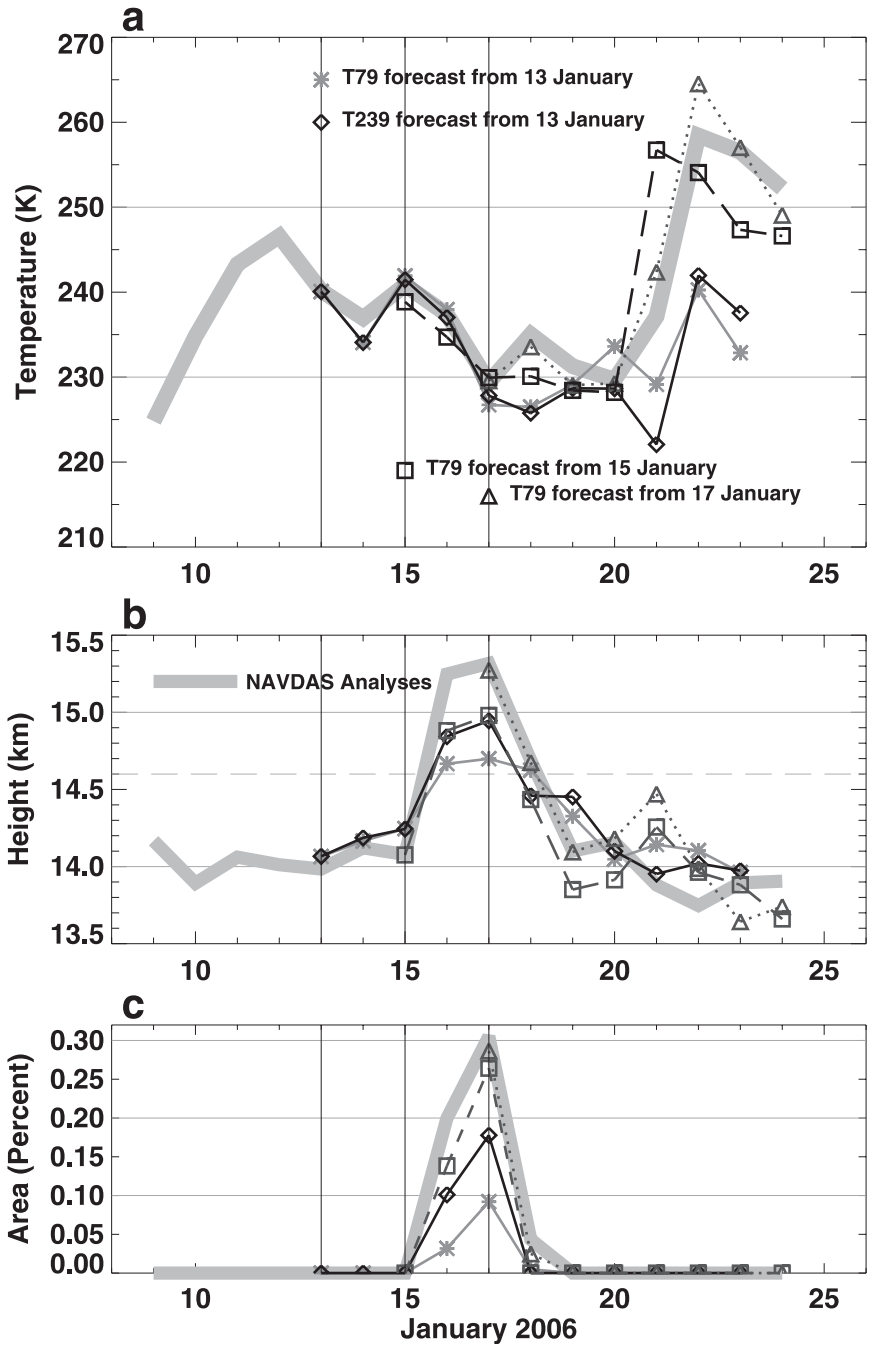


FIG. 8. (a) Temperature (K) at 10 hPa averaged poleward of 80°N; (b) maximum 360-K potential temperature surface heights (km) between 45° and 55°N; (c) area (percent of globe) with 360-K potential temperature surface heights greater than 14.6 km between 45° and 55°N for 0000 UTC 9–24 Jan 2006. The thick gray curve denotes NOGAPS-ALPHA analyses. The asterisks, squares, and triangles denote T79 horizontal resolution forecasts initialized on 13, 15, and 17 Jan 2006, respectively. The diamonds denote a T239 horizontal resolution forecast initialized on 13 Jan 2006.

flow regions will determine the sign of the zonally averaged momentum flux. Thus, the zonally averaged results can be seen in the (nonzonally averaged) synoptic PV maps.

In summary, the main poleward transport during the subtropical wave breaking event of January 2006 was found to be limited to ~10 km or less in altitude, centered near 10 hPa. This localized, poleward-moving PV

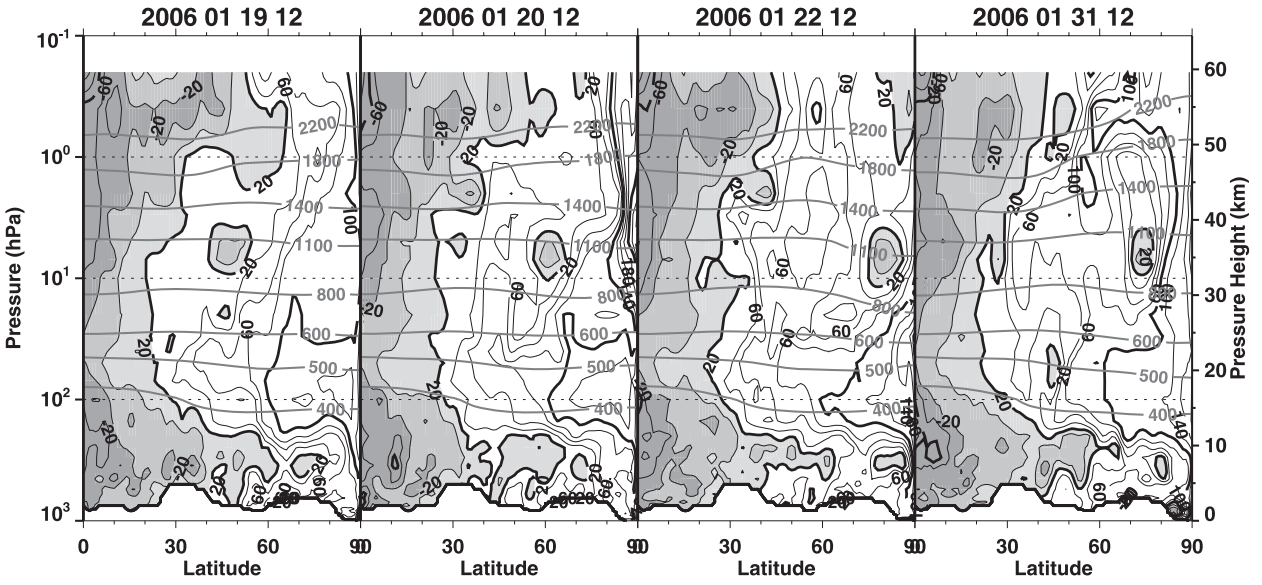


FIG. 9. The minimum absolute vorticity at each latitude and pressure for 19, 20, 22, and 31 Jan 2006. Contour interval is $20 \times 10^{-6}$ s$^{-1}$; low values are shaded. Gray contours show zonal averaged potential temperature at 400, 500, 600, 800, 1100, 1400, 1800, and 2200 K.

anomaly was shown to influence the zonally averaged winds and to focus the EP flux vectors poleward.

## 5. Discussion and conclusions

The middle atmosphere northern winter of 2005/06 was characterized by a disturbed stratospheric polar vortex culminating in a major SSW on 20 January 2006. As shown in section 3, a large upper tropospheric ridge formed over the North Atlantic (15–18 January), advecting a pool of lower tropospheric warm air to ~50°N. This warm air advection was compensated aloft by strong cooling, resulting in a large upward perturbation of the 360-K potential temperature surface that peaked on 16–17 January. This large 360-K surface perturbation (over 2 km above the mean value) was

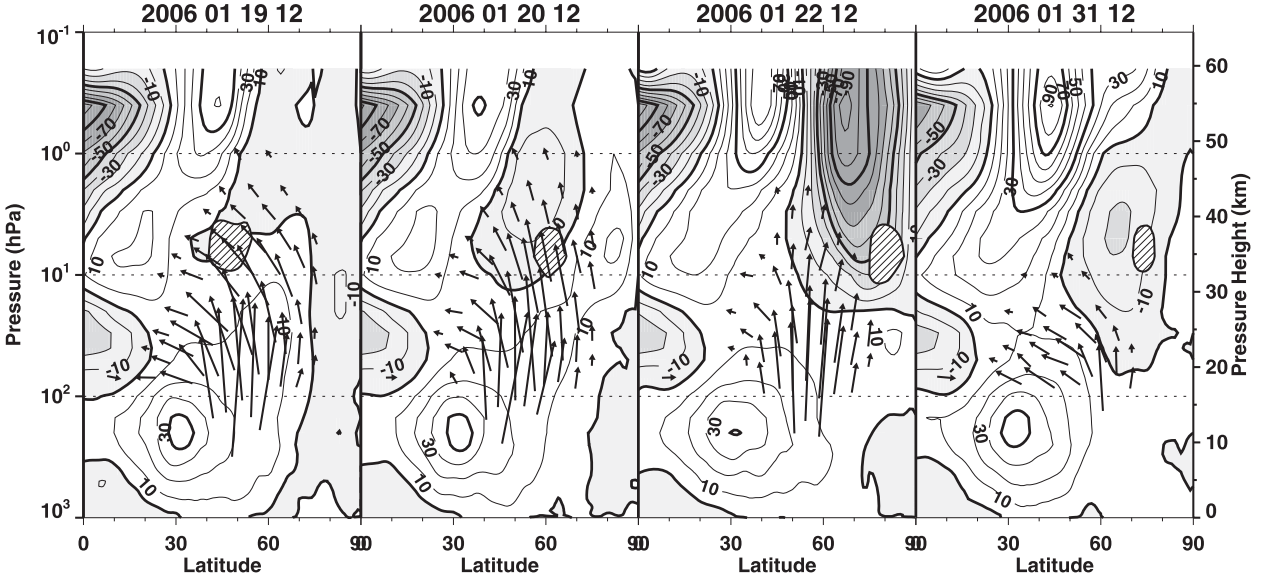


FIG. 10. The zonal average of zonal wind for 19, 20, 22, and 31 Jan 2006. Contour interval 10 m s$^{-1}$; easterly winds are shaded. The diagonally striped region is the minimum absolute vorticity contour of $20 \times 10^{-6}$ s$^{-1}$ taken from corresponding panels of Fig. 9. Arrows denote EP flux vectors above the tropopause.

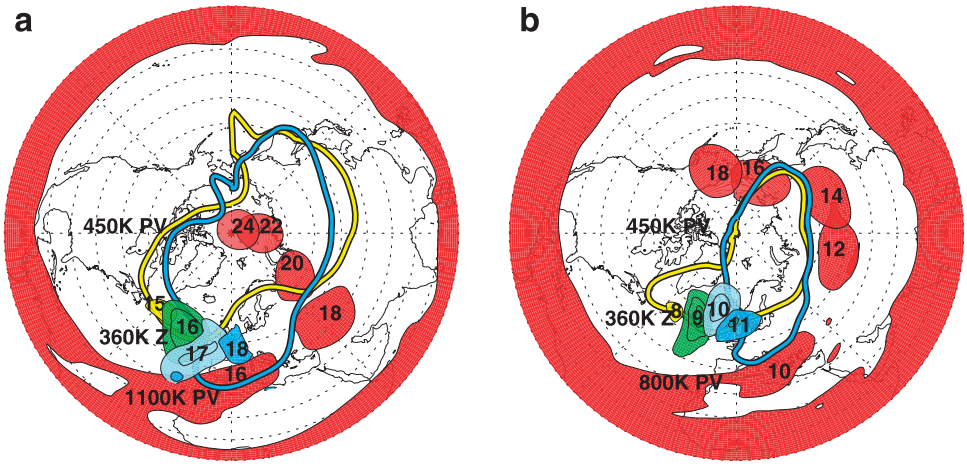


FIG. 11. Summary plots for (a) January 2006 and (b) January 2003 showing 360-K heights (yellow, green, light blue, and blue regions), 450-K PV (yellow and blue contours), and midstratosphere PV (red regions). The 360-K heights are for (a) 15–18 Jan 2006 with the lowest contour at 14.2 km, contour interval 0.4 km, and (b) 8–11 Jan 2003 with the lowest contour at 14.6 km, contour interval 0.4 km. The 450-K PV is contoured on (a) 15 (yellow) and 18 (blue) Jan 2006 at 20 PVU and (b) 8 (yellow) and 11 (blue) Jan 2003 at 28 PVU. The midstratospheric PV is at (a) 1100 K contoured at 250 PVU for 16, 18, 20, 22, and 24 Jan 2006 and (b) 800 K contoured at 100 PVU for 10, 12, 14, 15, and 18 Jan 2003.

associated with a region of strong EP flux divergence (a planetary wave source region) consisting of a strong upward vertical EP flux component. This strong upper troposphere–lower stratosphere system produced a record low total ozone value (177 DU) over the United Kingdom on 19 January (Keil et al. 2007). The rapid growth of this upper tropospheric disturbance and its extension into the lower stratosphere (Fig. 6) suggest that a resonant instability may be occurring (see discussion in McIntyre 1982). After the major warming, planetary wave activity decreased in the upper stratosphere and the stratopause disappeared, only to reform at much higher altitude and slowly descend during February (Siskind et al. 2007; Manney et al. 2008).

Further investigation is needed to determine what fraction of SSWs is initiated by localized upper tropospheric forcing. However, an examination of the maximum values of 360-K potential temperature height in the 40°–50°N latitude range for the years 1991–2006 (December–February months taken from Met Office analyses; not shown) finds that January 2006 and January 2003 had the two largest values during this time period. As in January 2006, the January 2003 maximum also occurred prior to a major SSW. Figure 11 shows a summary comparison of the January 2006 and January 2003 stratospheric warming events. In both events a sudden increased in 360-K heights over the North Atlantic is accompanied by changes in the lower stratosphere (450-K PV) vortex above the North Atlantic and by wave breaking in the midstratosphere. In both cases, the large upper troposphere disturbance amplifies under the 450-K vortex winds (the vortex edge region; see Fig. 5). In both events the elevated 360-K surfaces are associated with very low total ozone (so-called ozone minihole; see McCormack et al. 2004 for a discussion of ozone minihole formation during the January 2003 event).

Another example of strong localized upper tropospheric forcing followed by tropical wave breaking occurred over the South Atlantic prior to the major SSW of September 2002 (Allen et al. 2006). Although this upper troposphere forcing has been characterized as blocking (Nishii and Nakamura 2004), it exhibited a horizontal scale and eastward propagation similar to that presented here for January 2006. As in the January 2006 case, Nishii and Nakamura (2004) showed that this upper tropospheric forcing was accompanied by a horizontally localized elevated tropopause and strong vertical EP fluxes. An initial examination of analyses for September 2002 has found that this tropospheric forcing event was followed by a stratospheric tropical wave breaking event over the South Atlantic. Although this tropical wave breaking likely played an important role in the SSW, additional dynamics and wave breaking may be involved in this complex case (Harnik et al. 2005).

The forecasting experiments (Fig. 8) show, in this case, the importance of accurately forecasting the upper tropospheric disturbance prior to forecasting the major sudden warming. A major warming similar to the January

2006 major warming only occurred in the model when preceded by a realistic forecast or initialization of the large area anomaly in the North Atlantic upper troposphere. A similar result, highlighting the importance of forecasting the upper tropospheric blocking event that led to the September 2002 SSW, was reported by Allen et al. (2006).

We have shown that local diagnostics—such as the height of the 360-K potential temperature surface, the 100-hPa meridional heat flux, or 100-hPa temperatures (curves a, b, and c in Fig. 3)—can, in some cases, be much better than geopotential heights or zonal average quantities in identifying the large-amplitude upper tropospheric disturbances that are capable of producing dramatic changes in the stratospheric vortex. Large changes in these local diagnostics that occur below the lower stratospheric vortex (such as in Fig. 5) seem to be especially effective in producing large dynamical changes in the stratosphere. In addition, whereas previous studies (e.g., Taguchi 2008) have examined forcing with synoptic waves filtered out, we have found that synoptic systems (~zonal wavenumbers 4–5) are capable of directly forcing SSWs and should be considered when searching for tropospheric–SSW connections.

The subtropical wave breaking seen in January 2006 revealed a relatively shallow vertical structure. This is similar to the finding of O'Neill et al. (1994) in which they noted that the eastward/poleward propagating high pressure seen in the January 1992 minor SSW did not extend down to the lower stratosphere. The limited vertical extent of the developing anticyclone seen in January 2006 contrasts with generic warming simulations that show deep filaments of high-PV air during polar wave breaking events (Polvani and Saravanan 2000) and is probably not typical of most warmings. However, the limited vertical extent may be more typical of subtropical wave breaking events and hence may be an important factor in the amount of mixing during these events.

We examined how the local PV anomaly at 1100 K influenced the zonally averaged zonal wind and the EP flux vectors as it propagated poleward. This 1100-K PV anomaly (Fig. 1) resembled the nonlinear wave breaking reviewed in Andrews et al. (1987, see p. 256) at early times (16 January 2006), whereas at later times (20–22 January) the 100-K PV field more closely resembled interacting cyclonic and anticyclonic vortices (Scott and Dritschel 2006). Despite these highly nonlinear dynamics, the EP fluxes (Fig. 9) showed equatorward propagation followed by poleward propagation (Dunkerton et al. 1981), suggesting that the nonlinear wave breaking at the critical layer is acting to reflect wave energy and thus contribute to the poleward focusing of EP flux during the SSW. Thus, reflection from the subtropical wave breaking was a crucial component in the SSW of January 2006.

We plan on examining long-term reanalyses for additional examples of local upper tropospheric forcing and subtropical wave breaking. Diagnostics such as the minimum absolute vorticity as a function of latitude and altitude (Fig. 9) and/or midlatitude 360-K heights (Fig. 2) for other warmings will be fundamental for comparisons with the January 2006 warming, compositing studies, and predictability studies.

*Acknowledgments.* This research was supported by the Office of Naval Research and the NASA MAP program. We thank David Siskind, John McCormack, and Steven Pawson for their research insights and manuscript comments.

## REFERENCES

Allen, D. R., L. Coy, S. D. Eckermann, J. P. McCormack, G. L. Manney, T. F. Hogan, and Y.-J. Kim, 2006: NOGAPS-ALPHA simulations of the 2002 Southern Hemisphere stratospheric major warming. *Mon. Wea. Rev.,* **134,** 498–518.

Andrews, D. G., J. R. Holton, and C. B. Leovy, 1987: *Middle Atmosphere Dynamics.* Academic Press, 489 pp.

Bloom, S., and Coauthors, 2005: Documentation and validation of the Goddard Earth Observing System (GEOS) data assimilation system—Version 4. NASA Technical Report Series on Global Modeling and Data Assimilation 104606, Vol. 26, 187 pp. [Available online at http://gmao.gsfc.nasa.gov/systems/geos4/Bloom.pdf.]

Charney, J. G., and P. G. Drazin, 1961: Propagation of planetary-scale disturbances from the lower into the upper atmosphere. *J. Geophys. Res.,* **66,** 83–109.

Dunkerton, T., C.-P. F. Hsu, and M. E. McIntyre, 1981: Some Eulerian and Lagrangian diagnostics for a model stratospheric warming. *J. Atmos. Sci.,* **38,** 819–843.

Eckermann, S. D., J. P. McCormack, L. Coy, D. Allen, T. Hogan, and Y.-J. Kim, 2004: NOGAPS-ALPHA: A prototype high-altitude global NWP model. Preprints, *Symp. 50th Anniversary of Operational Numerical Weather Prediction,* College Park, MD, Amer. Meteor. Soc., P2.6.

——, and Coauthors, 2008: High-altitude data assimilation system experiments for the Northern Hemisphere summer mesosphere season of 2007. *J. Atmos. Solar-Terr. Phys.,* doi:10.1016/jojastp.2008.09.036, in press.

Goerss, J. S., and P. A. Phoebus, 1992: The Navy's operational atmospheric analysis. *Wea. Forecasting,* **7,** 232–249.

Harnik, N., R. K. Scott, and J. Perlwitz, 2005: Wave reflection and focusing prior to the major stratospheric warming of September 2002. *J. Atmos. Sci.,* **62,** 640–650.

Haynes, P., 2005: Stratospheric dynamics. *Annu. Rev. Fluid Mech.,* **37,** 263–293.

Hogan, T., and T. Rosmond, 1991: The description of the Navy Operational Global Atmospheric Prediction System's spectral forecast model. *Mon. Wea. Rev.,* **119,** 1786–1815.

Hoppel, K. W., N. L. Baker, L. Coy, S. D. Eckermann, J. P. McCormack, G. E. Nedoluha, and D. E. Siskind, 2008:

Assimilation of stratospheric and mesospheric temperatures from MLS and SABER into a global NWP model. *Atmos. Chem. Phys.,* **8,** 6103–6116.

Keil, M., D. R. Jackson, and M. C. Hort, 2007: The January 2006 low ozone event over the UK. *Atmos. Chem. Phys.,* **7,** 961–972.

Killworth, P. D., and M. E. McIntyre, 1985: Do Rossby-wave critical layers absorb, reflect or over-reflect? *J. Fluid Mech.,* **161,** 449–492.

Lait, L. R., 1994: An alternative form for potential vorticity. *J. Atmos. Sci.,* **51,** 1754–1759.

Limpasuvan, V., D. W. J. Thompson, and D. L. Hartmann, 2004: The life cycle of the Northern Hemisphere sudden stratospheric warmings. *J. Climate,* **17,** 2584–2596.

Manney, G., and Coauthors, 2008: The evolution of the stratopause during the 2006 major warming: Satellite data and assimilated meteorological analyses. *J. Geophys. Res.,* **113,** D11115, doi:10.1029/2007JD009097.

McCormack, J. P., and Coauthors, 2004: NOGAPS-ALPHA model simulations of stratospheric ozone during the SOLVE2 campaign. *Atmos. Chem. Phys.,* **4,** 2401–2423.

McIntyre, M. E., 1982: How well do we understand the dynamics of stratospheric warmings? *J. Meteor. Soc. Japan,* **60,** 37–65.

Nishii, K., and H. Nakamura, 2004: Tropospheric influence on the diminished Antarctic ozone hole in September 2002. *Geophys. Res. Lett.,* **31,** L16103, doi:10.1029/2004GL019532.

O'Neill, A., W. L. Grose, V. D. Pope, H. Maclean, and R. Swinbank, 1994: Evolution of the stratosphere during northern winter 1991/92 as diagnosed from the U.K. Meteorological Office analyses. *J. Atmos. Sci.,* **51,** 2800–2817.

Polvani, L. M., and R. Saravanan, 2000: The three-dimensional structure of breaking Rossby waves in the polar wintertime stratosphere. *J. Atmos. Sci.,* **57,** 3663–3685.

——, D. W. Waugh, and R. A. Plumb, 1995: On the subtropical edge of the stratospheric surf zone. *J. Atmos. Sci.,* **52,** 1288–1309.

Randel, W. J., J. C. Gille, A. E. Roche, J. B. Kumer, J. L. Mergenthaler, J. W. Waters, E. F. Fishbein, and W. A. Lahoz, 1993: Stratospheric transport from the tropics to middle latitudes by planetary-wave mixing. *Nature,* **365,** 533–535.

Scott, R. K., and D. G. Dritschel, 2006: Vortex–vortex interactions in the winter stratosphere. *J. Atmos. Sci.,* **63,** 726–740.

Siskind, D. E., S. D. Eckermann, L. Coy, J. P. McCormack, and C. E. Randall, 2007: On recent interannual variability of the Arctic winter mesosphere: Implications for tracer descent. *Geophys. Res. Lett.,* **34,** L09806, doi:10.1029/2007GL029293.

Taguchi, M., 2008: Is there a statistical connection between stratospheric sudden warming and tropospheric blocking events? *J. Atmos. Sci.,* **65,** 1442–1454.

Waugh, D. W., 1993: Subtropical stratospheric mixing linked to disturbances in the polar vortices. *Nature,* **365,** 535–537.